

RESEARCH ARTICLE

# A genome-wide association study reveals a novel regulator of ovule number and fertility in *Arabidopsis thaliana*

Jing Yuan <sup>1,2</sup>, Sharon A. Kessler <sup>1,2\*</sup>

**1** Department of Botany and Plant Pathology, Purdue University, West Lafayette, Indiana United States of America, **2** Purdue Center for Plant Biology, Purdue University, West Lafayette, Indiana United States of America

\* [sakessler@purdue.edu](mailto:sakessler@purdue.edu)



 OPEN ACCESS

**Citation:** Yuan J, Kessler SA (2019) A genome-wide association study reveals a novel regulator of ovule number and fertility in *Arabidopsis thaliana*. PLoS Genet 15(2): e1007934. <https://doi.org/10.1371/journal.pgen.1007934>

**Editor:** Esther van der Knaap, University of Georgia, UNITED STATES

**Received:** August 1, 2018

**Accepted:** January 4, 2019

**Published:** February 11, 2019

**Copyright:** © 2019 Yuan, Kessler. This is an open access article distributed under the terms of the [Creative Commons Attribution License](https://creativecommons.org/licenses/by/4.0/), which permits unrestricted use, distribution, and reproduction in any medium, provided the original author and source are credited.

**Data Availability Statement:** All relevant data are within the manuscript and its Supporting Information files.

**Funding:** This work was funded by Purdue University Start-up funds to S.A.K. and a grant from the Oklahoma Center for the Advancement of Science and Technology (<https://www.ok.gov/ocast/>) #PS14-008 to S.A.K. The funders had no role in study design, data collection and analysis, decision to publish, or preparation of the manuscript.

## Abstract

Ovules contain the female gametophytes which are fertilized during pollination to initiate seed development. Thus, the number of ovules that are produced during flower development is an important determinant of seed crop yield and plant fitness. Mutants with pleiotropic effects on development often alter the number of ovules, but specific regulators of ovule number have been difficult to identify in traditional mutant screens. We used natural variation in *Arabidopsis* accessions to identify new genes involved in the regulation of ovule number. The ovule numbers per flower of 189 *Arabidopsis* accessions were determined and found to have broad phenotypic variation that ranged from 39 ovules to 84 ovules per pistil. Genome-Wide Association tests revealed several genomic regions that are associated with ovule number. T-DNA insertion lines in candidate genes from the most significantly associated loci were screened for ovule number phenotypes. The *NEW ENHANCER of ROOT DWARFISM (NERD1)* gene was found to have pleiotropic effects on plant fertility that include regulation of ovule number and both male and female gametophyte development. Overexpression of *NERD1* increased ovule number per fruit in a background-dependent manner and more than doubled the total number of flowers produced in all backgrounds tested, indicating that manipulation of *NERD1* levels can be used to increase plant productivity.

## Author summary

Ovules are the precursors of seeds in flowering plants. Each ovule contains an egg cell and a central cell that fuse with two sperm cells during double fertilization to generate seeds containing an embryo and endosperm. The number of ovules produced during flower development determines the maximum number of seeds that can be produced by a flower. In this paper, we used natural variation in *Arabidopsis thaliana* accessions to identify regions of the genome that are associated with ovule number. Polymorphisms in the plant-specific *NERD1* gene on chromosome 3 were significantly associated with ovule number. Mutant and overexpression analyses revealed that *NERD1* is a positive regulator

**Competing interests:** The authors have declared that no competing interests exist.

of ovule number, lateral branching, and flower number in *Arabidopsis*. Manipulation of NERD1 expression levels could potentially be used to increase yield in crop plants.

## Introduction

During plant reproduction, pollen tubes deliver two sperm cells to female gametophytes contained within ovules. This allows double fertilization to occur in order to produce the embryo and endosperm in the developing seed. Angiosperms with all kinds of pollination syndromes (insect-, wind-, and self-pollinated) produce much more pollen than ovules in order to ensure successful pollination. For example, most soybean varieties produce only 2 ovules per flower, but more than 3,000 pollen grains, a 1,500-fold difference[1]. Wind-pollinated plants such as maize have an even more extreme difference in pollen production vs. ovule production per plant, with more than 1 million pollen grains versus an average of 250 ovules per plant (a 4000-fold difference[2]). *Arabidopsis thaliana*, which is a self-pollinating plant, also produces an excess of pollen, with at least 2000 pollen grains per flower compared to an average of 60 ovules per flower[3]. Since pollen is produced in excess, in self-pollinated plants the number of ovules (i.e. female gametes) sets the maximum seed number per flower.

The ability to manipulate ovule number to increase the reproductive potential of plants requires an understanding of the molecular pathways that control ovule initiation. The model plant *Arabidopsis thaliana* produces flowers with four whorls of organs: sepals, petals, stamens, and carpels. The inner whorls (3 and 4) are responsible for sexual reproduction, with pollen (the male gametophytes) produced in the whorl 3 stamens and the female gametophytes (also known as the embryo sacs), produced in ovules contained within the whorl 4 carpels. Specification of the 4 whorls is controlled by the “ABC” genes, with the C-class gene AGAMOUS (AG) a major regulator of carpel development[4].

In *Arabidopsis*, ovules are initiated from the carpel margin meristem (CMM) at stage 9 of floral development[5]. The *Arabidopsis* gynoecium comprises two carpels that are fused vertically at their margins [6]. The CMM develops on the adaxial face of the carpels (inside the fused carpel cylinder) and will give rise to the placenta, ovules, septum, transmitting tract, style, and stigma. Once the placenta is specified, all of the ovule primordia are initiated at the same time[7]. Subsequently, each primordium will be patterned into three different regions: the funiculus, which connects the ovule to the septum; the chalaza, which gives rise to the integuments; and the nucellus, which gives rise to the embryo sac. Ovule development concludes with the specification of the megaspore mother cell within the nucellus which undergoes meiosis followed by three rounds of mitosis to form the mature haploid embryo sac (reviewed in[8]).

In *Arabidopsis*, CMM development requires coordination of transcriptional regulators involved in meristem function with hormone signaling (reviewed in[6]). Most mutants that have been reported to affect ovule number have pleiotropic effects related to the establishment of polarity and boundaries during gynoecial development (reviewed in [9]). For example, the *AINTEGUMENTA* (*ANT*) transcription factor regulates organ initiation and cell divisions during flower development[10]. *ANT* acts redundantly with the related gene *AINTEGUMENTA-LIKE6/PLETHORA3* to regulate carpel margin development and fusion which leads to a modest reduction in ovule number. This phenotype is exacerbated when *ant* is combined with mutations in other carpel development transcriptional regulators, such as *SEUSS* (*SEU*), *LEUNIG* (*LUG*), *SHATTERPROOF1* and *2* (*SHP1* and *SHP2*), *CRABSCLAW* (*CRC*),

*FILAMENTOUS FLOWER (FIL)*, and *YABBY3 (YAB3)*. Mutant combinations between *ant* and these mutants leads to severe defects in carpel fusion coupled with severe reductions in the marginal tissues that give rise to the CMM (summarized in [6]). An extreme example is the double mutant *seu-3 ant-1* which results in a complete loss of ovule initiation due to defects in CMM development [11]. The organ boundary genes, *CUP-SHAPED COTYLEDON1* and 2 (*CUC1* and *CUC2*), are also required for CMM development and subsequent ovule initiation. *ant cuc2* mutants with *cuc1* levels decreased specifically in the CMM by an RNAi construct driven by the *SEEDSTICK* promoter show an 80% reduction in ovule number, indicating that *ANT* controls cell proliferation while *CUC1/2* are necessary to set up the boundaries that allow ovule primordia to be initiated [12].

Plant hormones are also involved in gynoecium development and can have both indirect and direct effects on ovule number. Auxin biosynthesis, signaling, and transport mutants have varying effects on gynoecium development and patterning, many of which lead to pleiotropic effects on tissues and organs derived from the CMM [13]. Treatment of developing flowers with the auxin polar transport inhibitor NPA showed that an apical-basal auxin gradient in the developing gynoecium is necessary for patterning events that lead to ovule initiation [13]. Cytokinin has also been implicated in ovule initiation and development in *Arabidopsis*. Notably, triple mutants in the *ARABIDOPSIS HISTIDINE KINASE (AHK)* cytokinin receptors, *AHK2*, *AHK3*, and *AHK4/CRE1*, displayed a 90% reduction in ovule number due to decreased cytokinin signaling [14]. Conversely, double mutants in the cytokinin degrading cytokinin oxidases/dehydrogenases (CKXs) displayed higher cytokinin levels in inflorescences and produced more than double the number of ovules as in wild-type controls [15]. Brassinosteroids (BR) may also be positive regulators of ovule initiation. Gain-of-function mutants in the BR-induced transcription factor *BZR1* had increased ovule number per flower while BR-deficient and insensitive mutants had decreased ovule number compared to wild-type controls. Upregulation of the ovule regulators *ANT* and *HUELLENLOS (HLL)* was correlated with *BZR1* activity, indicating the BR signaling positively regulates ovule development [16]. Recently, gibberellins were shown to negatively regulate ovule number independently of auxin transport and signaling. A gain-of-function mutation in the *DELLA* gene, *GA-INSENSITIVE (GAI)* and loss-of-function mutations in GA receptors all led to increased ovule number in *Arabidopsis* [17].

To date, research on the factors controlling ovule number has been dominated by the analyses of mutants that have been identified based on pleiotropic effects on gynoecium development. In an attempt to identify loci that regulate ovule number without affecting other aspects of flower morphology, we took advantage of natural variation in ovule number in *Arabidopsis* accessions from diverse geographical locations. Over 7,000 natural accessions are now available with intraspecific variation, and next generation sequencing has been used to generate data on single nucleotide polymorphisms (SNPs) from over 1,000 of these accessions as part of the 1001 genomes project [18]. 100s of different phenotypes have been analyzed in this collection such as flowering time, leaf shape and size, the ability to resist to pathogens, etc. [19]. In this study, we identified variation in ovule number per flower in a screen of 189 *Arabidopsis* accessions and conducted a Genome Wide Association Study (GWAS) to identify loci associated with the ovule number trait. Further analysis of two loci identified in our GWAS revealed that the *NEW ENHANCER of ROOT DWARFISM (NERD1)* and *OVULE NUMBER ASSOCIATED 2 (ONA2)* genes participate in the determination of ovule number during *Arabidopsis* flower development. The discovery of new ovule number regulators in *Arabidopsis* has the potential to provide targets for the development of crop varieties with greater yield.

## Results

### Natural variation in ovule number

We set out to identify new regulators of ovule number in *Arabidopsis* by taking advantage of phenotypic variation in naturally occurring accessions. We obtained 189 *Arabidopsis* accessions from the ABRC and assayed them for variation in ovule number (S1 Table). Since ovule number can vary throughout the life cycle of the plant[20], we determined the average number of ovules from flowers 6–10 on the main stem of plants that were vernalized for 4 weeks and then grown in long days at 22°C. Under these growth conditions, accessions displayed a remarkable diversity in ovule number per flower, with a range of 39–82 ovules per flower (Fig 1A and 1B). The commonly used reference accession, Col-0, falls in the middle of the range with an average ovule number of  $63 \pm 3$  ovules.

In contrast to flowering time variation which has been shown to correlate with latitude of origin in *Arabidopsis* accessions[21], ovule number was not strongly correlated with location of origin in the accessions analyzed (Figs 1C and S1). Mapping ovule number data onto a cladogram of the accessions used in our study revealed a cluster of low ovule number accessions in one specific clade, indicating that these closely-related accessions may have similar genetic control of ovule number (Fig 1D). Interestingly, several clades were made up of accessions with high, medium, and low ovule numbers. This suggests that the ovule number trait may be regulated by different loci that have been selected for in some lineages.

### GWAS reveals SNPs linked to natural variation in ovule number

In order to identify genomic regions linked to variation in ovule number, we assessed whether the average ovule number per flower from 148 accessions was predicted by Single Nucleotide Polymorphisms (SNP) available in the 1001 Full-sequence dataset; TAIR 9. Logarithmic transformation was applied to the ovule number data to make the results more reliable for parametric tests. Associations were tested for each SNP using a linear regression model (LM) and the results were analyzed using GWAPP[22] (Fig 2A). A significance cutoff value of  $-\log_{10}(p \text{ values}) \geq 6.2$  identified at least 9 genomic regions that are associated with variation in ovule number, while a higher cutoff of  $-\log_{10}(p \text{ values}) \geq 7.5$  identifies only four significant genomic regions.

We next determined if known ovule number regulators [9, 15, 17, 23] colocalized with our GWAS loci. Of the previously described loci, only BIN2 mapped close to a significant association (S2 Fig). This indicates that our GWAS has identified novel functions for loci in the regulation of ovule number. For further analysis, we focused on the two loci with the lowest p-values which are both located on the long arm of chromosome 3 (Fig 2B and 2C). Genes containing the most significantly associated SNPs as well as the 10 surrounding genes around the highest peak were considered as candidates for regulating ovule number. These genes were further prioritized based on whether they are expressed in developing pistils, by examining publicly available transcriptome data in ePlant[24] (S3 Fig). Based on this prioritization, 35 candidate genes were selected, and of these 26 insertion mutants were available from the *Arabidopsis* Biological Resource Center. All 26 mutants were evaluated for changes in ovule number compared to the wild-type background, Col-0 (S2 Table). Of these, two had significantly reduced ovule number compared to the Col-0 control (Figs 3A and S4). The strongest ovule number phenotype was found in insertion mutants in At3g51050, a gene that was recently identified in a screen for enhancers of exocyst-mediated root phenotypes and named *NEW ENHANCER OF ROOT DWARFISM 1 (NERD1)*[25]. The second locus with T-DNA insertions affecting ovule number identified in our screen was At3g60660, which we call *OVULE NUMBER ASSOCIATED 2 (ONA2)*. *ONA2* encodes an unknown protein containing a DUF1395 domain (TAIR) (Fig 2C).

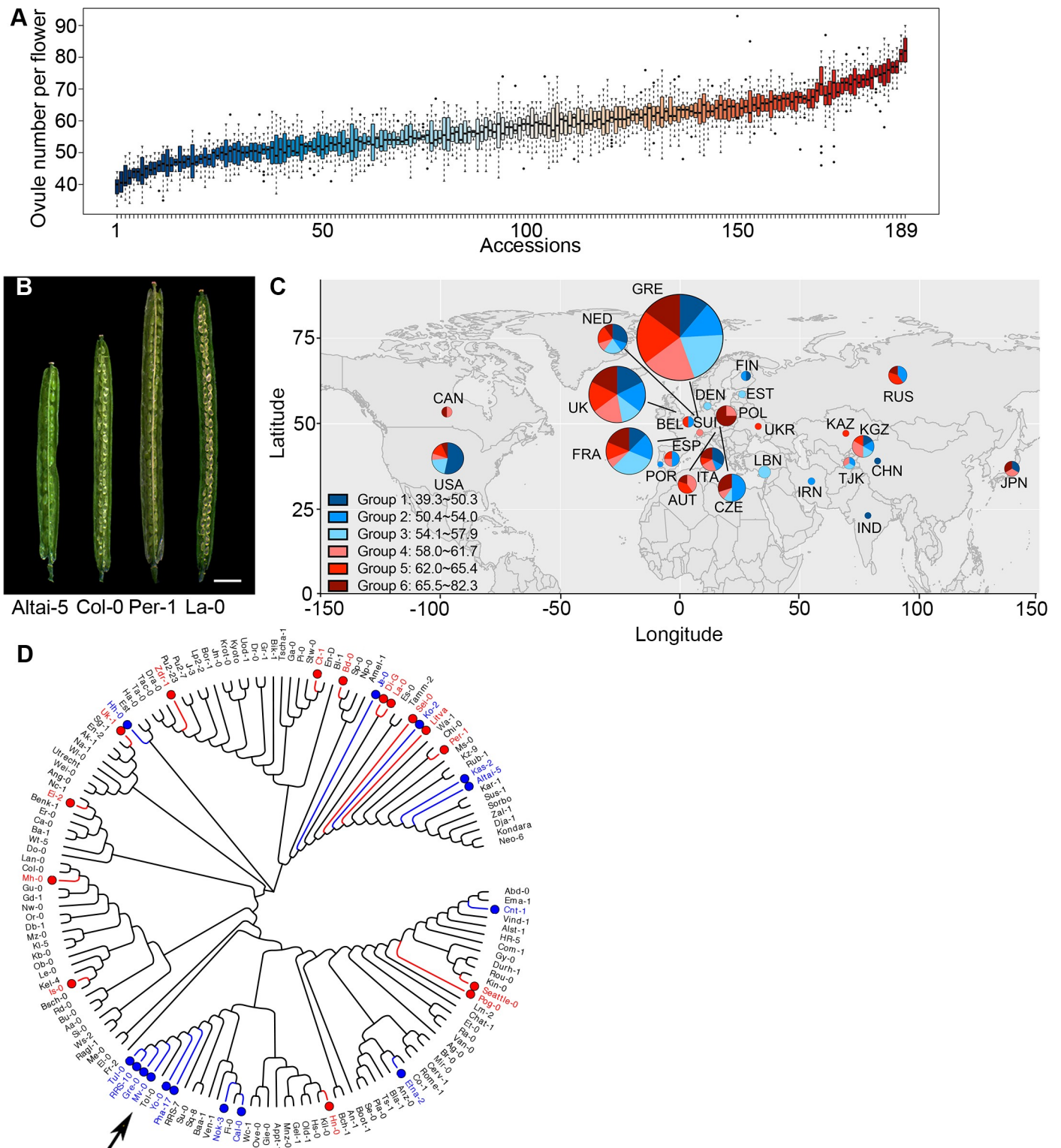


**Fig 1. Arabidopsis accessions display natural variation in ovule number per flower.** (A) Boxplot of ovule number in 189 Arabidopsis accessions. The detailed names of these accessions are in S1 Table. (B) Dissected siliques of low, medium, and high ovule number accessions (Bar = 2.0mm). (C) Geographic distribution of accessions. Groups 1 to 6 correspond to ovule number ranking (from low to high), with the colors corresponding to panel A. The pie chart indicates the percentage of accessions in each country in each ovule number group, while the size of the pie chart corresponds to the total number of accessions per country. (D) Cladogram of accessions used in this study (generated in MEGA7). The 15 accessions labeled in blue had the lowest ovule numbers, and the 15 accessions labeled with red had the highest ovule numbers. The arrow points to a clade with clustered low ovule number accessions.

<https://doi.org/10.1371/journal.pgen.1007934.g001>

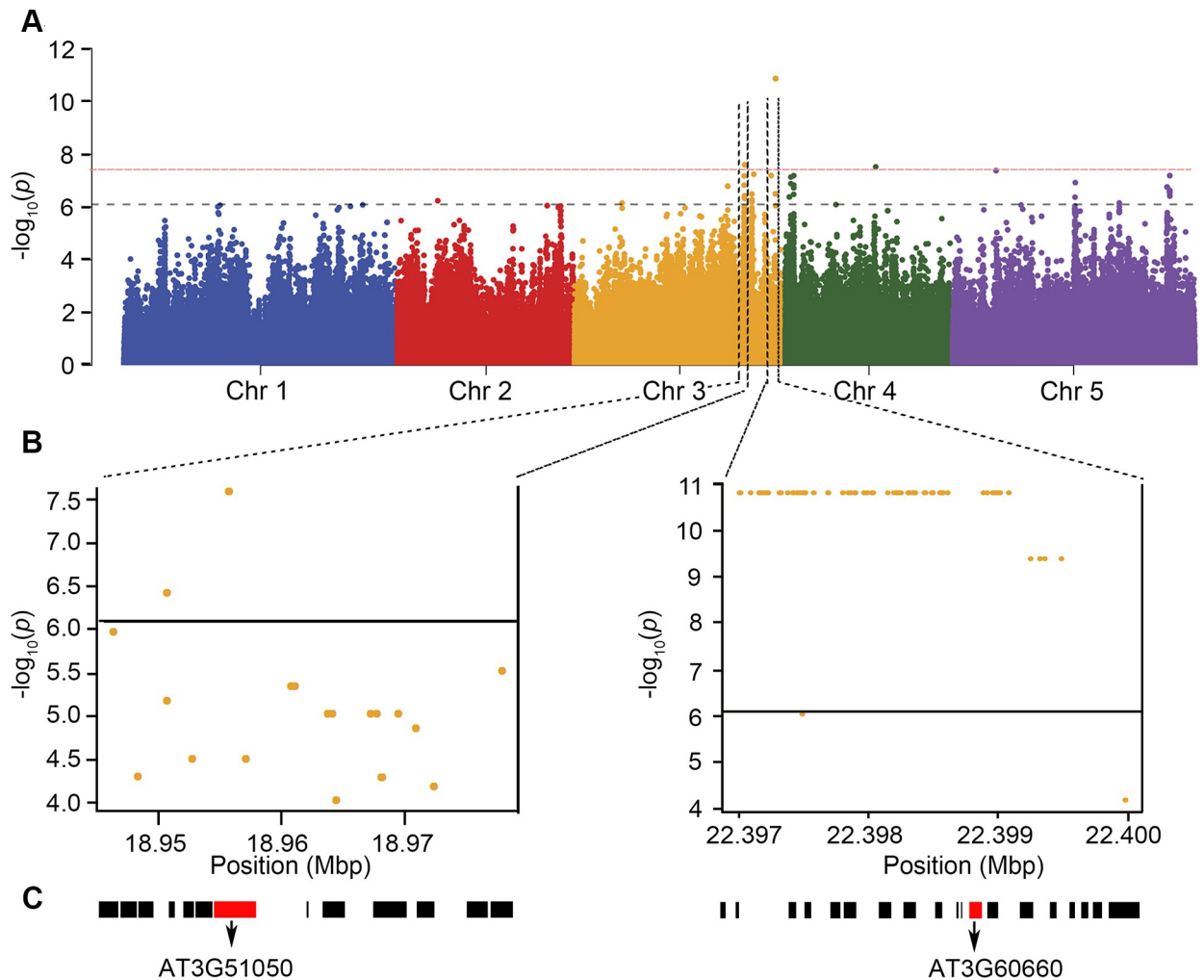


**Fig 2. GWAS identifies candidate loci associated with ovule number per flower.** (A) Manhattan plot for the SNPs associated with ovule number per flower. Chromosomes are depicted in different colors. The horizontal blue dashed line corresponds to  $-\log_{10}(p)$  values  $\geq 6.2$  and the red dashed line corresponds to  $-\log_{10}(p)$  values  $\geq 7.5$  after Benjamini Hochberg (False Discovery Rate) correction. (B) The genomic region surrounding the two most significant GWA peaks on Chromosome 3. (C) Genes in the genomic region surrounding the two significant GWA peaks in (B). The red boxes are AT3G51050 (*NERD1*) and AT3G60660 (*ONA2*).

<https://doi.org/10.1371/journal.pgen.1007934.g002>

### ***NERD1* is a positive regulator of ovule number**

We focused our analysis on *NERD1* since it had the strongest effect on ovule number. The fruits of homozygous mutants in two T-DNA insertion alleles, *nerd1-2* (described in [25] and *nerd1-4*, had fewer ovules than wild-type plants (Fig 3A). To confirm that this resulted from the disruption of *NERD1*, we generated transgenic plants expressing a translational fusion of the *NERD1* protein with the red-fluorescent protein tdTomato under the control of the native *NERD1* promoter. In *nerd1-2* and *nerd1-4* mutants, this transgene fully rescued the reduced ovule phenotype and resulted in plants with ovule numbers indistinguishable from Col-0 (Fig 3A). This demonstrates that *NERD1* is a positive regulator of ovule number.

In addition to reduced ovule number per flower, homozygous *nerd1* mutants had fertility defects. Homozygous *nerd1-2* mutants had 100% unfertilized ovules and homozygotes of the less severe *nerd1-4* allele had 75% unfertilized ovules (Figs 3B, 3C and S5A). *nerd1* mutants displayed both male and female defects. Homozygous *nerd1-2* mutants pollinated with Col-0

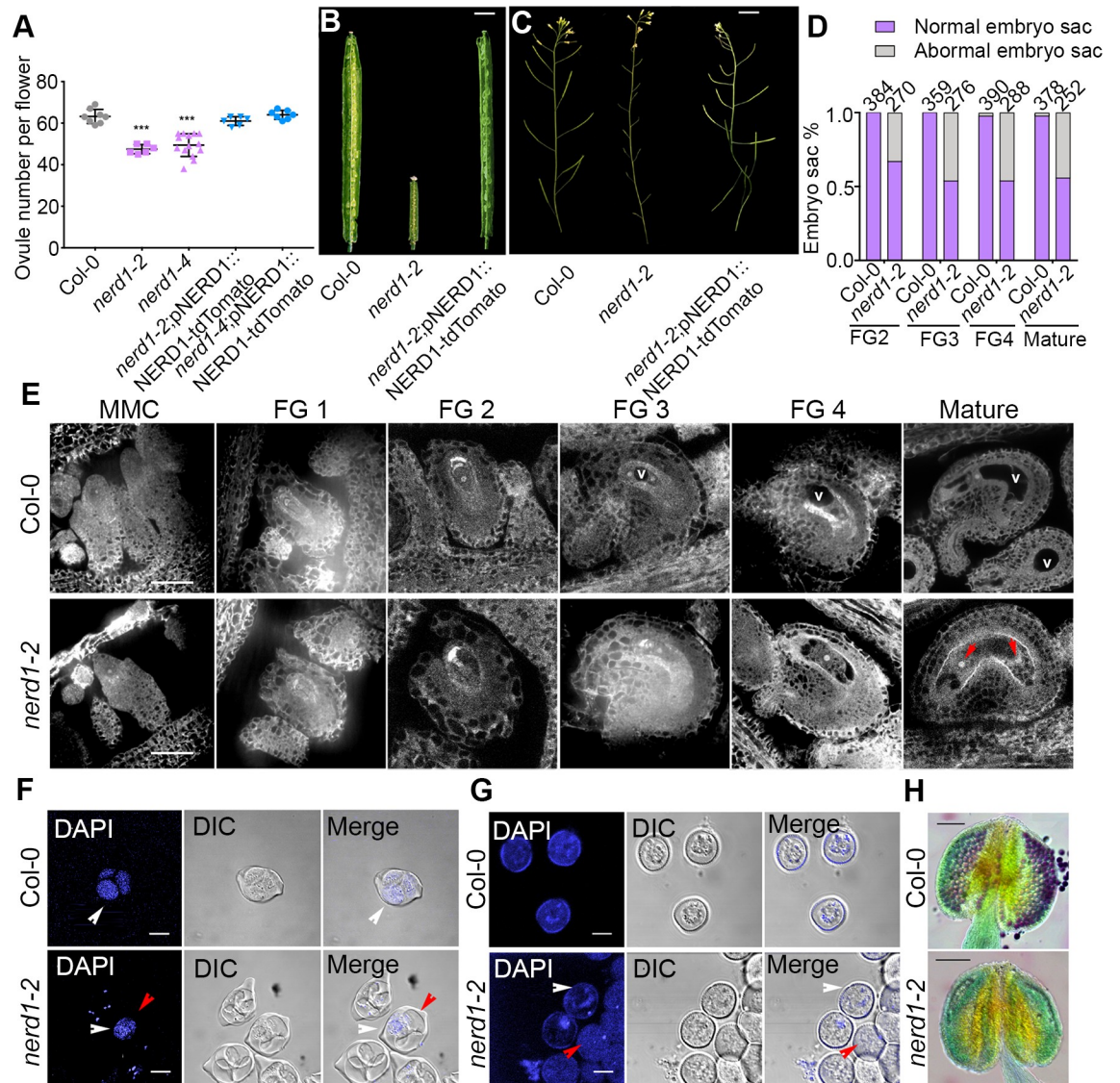


**Fig 3. *nerd1* mutants have reduced ovule number and fertility.** (A) Scatter plot of ovule number per flower in Col-0, *nerd1-2*, *nerd1-4* and their complementation lines. “\*\*\*\*” indicates statistical significance ( $p$  value < 0.001 determined by Student’s t-test). (B-C) *nerd1-2/nerd1-2* displays lower ovule number, infertile ovules, and short siliques compared to Col-0 and complemented lines. (D) Quantification of normal vs abnormal embryo sacs from developmental stages FG2 to mature ovules in Col-0 vs *nerd1-2/nerd1-2*. (E) During female gametophyte development, instead of the functional megaspore developing into female gametophyte by sequential mitotic divisions as seen in Col-0, *nerd1-2/nerd1-2* displays defective embryo sacs from stages FG2 to mature ovule. The central vacuole (V) is absent in FG3 and FG4 *nerd1* embryo sacs and mature ovules often have only 2 nuclei (red arrows) (F-G) DAPI staining of early stages of pollen development. (F) At tetrad stage in pollen development, *nerd1-2/nerd1-2* only has one developed haploid microspores instead of four microspores in Col-0 (white arrowheads indicate normal microspores and red arrowheads indicate aborted microspores). (G) After separation of the microspores, Col-0 has microspores with decondensed chromosomes, while most *nerd1-2/nerd1-2* microspores appear empty (white arrow heads indicate some normal chromosomes and red arrow head indicate empty microspores). (H) Alexander-stained Col-0 anthers have viable pollen grains (red indicates viable pollen while the green is non-viable). Alexander-stained *nerd1-2/nerd1-2* anthers have no viable pollen. Bars = 2.5mm (B-C), 30 $\mu$ m (E), 10 $\mu$ m (F-G), 100 $\mu$ m (H).

<https://doi.org/10.1371/journal.pgen.1007934.g003>

pollen displayed around 40% unfertilized ovules, indicating a female defect (S5A Fig). A developmental analysis of embryo sac development in homozygous *nerd1-2* mutants revealed that 38% embryo sacs were abnormal, with defects visible as early as the first mitosis (stage FG2) and mature ovules having a range of defects from only having 2 nuclei to complete collapse of

**Table 1. *nerd1* segregation in F2 populations.**

Allele	n	<i>NERD1</i> / <i>NERD1</i>	<i>nerd1</i> / <i>NERD1</i>	<i>nerd1</i> / <i>nerd1</i>	Expected ratio	$\chi^2$	p value
<i>nerd1-2</i>	107	35	49	23	1:2:1	3.4486	0.1783
<i>nerd1-4</i>	86	25	42	19	1:2:1	0.8837	0.6428

<https://doi.org/10.1371/journal.pgen.1007934.t001>

the embryo sac (Figs 3D, 3E, S5A and S6A). Pollen tube attraction to ovules requires proper differentiation of the embryo sac since the synergid cells secrete the LURE pollen tube attractants [26, 27]. The defective embryo sacs in *nerd1-2* mutants do not appear to differentiate the synergid, egg, and central cells necessary for double fertilization. Consistent with the defects in embryo sac development, only 41% of ovules attracted pollen tubes in *nerd1-2* pistils pollinated with Col-0 pollen (S5B and S5C Fig). Homozygous *nerd1-4* mutants displayed similar defects in embryo sac development, but a higher percentage of embryo sacs differentiated normally (S7A and S7B Fig).

Pollen development is also defective in *nerd1* mutants. During pollen development, the microspore mother cell undergoes meiosis to form a tetrad of four microspores. Tetrads were produced in *nerd1-2/nerd1-2* anthers, but 3 out of the four microspores collapsed and appeared to be aborted in mutant tetrads (Fig 3F). In the *nerd1-2* allele, later stages of pollen development were also defective and no viable pollen grains could be detected in mature anthers (Figs 3G, 3H and S6B). The less severe *nerd1-4* allele displayed similar defects in pollen development, but, similar to embryo sac development in both alleles, some normal pollen grains were produced (S7C and S7D Fig).

Both *nerd1-2* and *nerd1-4* segregate as recessive mutations in a 1:2:1 ratio in F2 populations (Table 1). This suggests that the male and female reproductive defects are sporophytic rather than gametophytic. To test this, we performed reciprocal crosses between heterozygous *nerd1-2* mutants and Col-0 wild-type plants (Table 2). When heterozygous *nerd1-2/NERD1* was used as the female, there was no transmission defect, demonstrating that the reduced female fertility in *nerd1-2* mutants was not female gametophytic. When *nerd1-2/NERD1* was used as the pollen donor, the transmission efficiency of the mutant allele was reduced to 45%, indicating a partial male gametophytic transmission defect (Table 2). Even though the *nerd1* F2 segregation ratios fit a 1:2:1 segregation by a *Chi*-squared test, it should be noted that the number of homozygous *nerd1* individuals is lower than wild-type individuals in both alleles (Table 1), consistent with a mild male gametophytic transmission defect.

### ***NERD1* encodes an integral membrane protein**

Phylogenetic analyses indicate that *NERD1* is a member of a low-copy number, highly conserved gene family that is found throughout the plant kingdom and in cyanobacteria (Fig 4A and 4B and [25]). The *NERD1* protein is predicted to be an integral membrane protein with a signal peptide and one transmembrane domain (Fig 5A). The majority of the protein is

**Table 2. Transmission efficiency of the *nerd1-2* allele determined by reciprocal crosses with wild-type Col-0.**

Female	Male	<i>NERD1</i> / <i>NERD1</i>	<i>nerd1-2</i> / <i>NERD1</i>	Female TE%	Male TE%	Chi-square test (p value)
<i>nerd1-2</i> / <i>NERD1</i>	Col-0	43	42	97.67	NA	0.91
Col-0	<i>nerd1-2</i> / <i>NERD1</i>	92	41	NA	44.57	9.767e <sup>-06</sup> *

\* Chi-square is significant at the p value < 0.01 level.

<https://doi.org/10.1371/journal.pgen.1007934.t002>

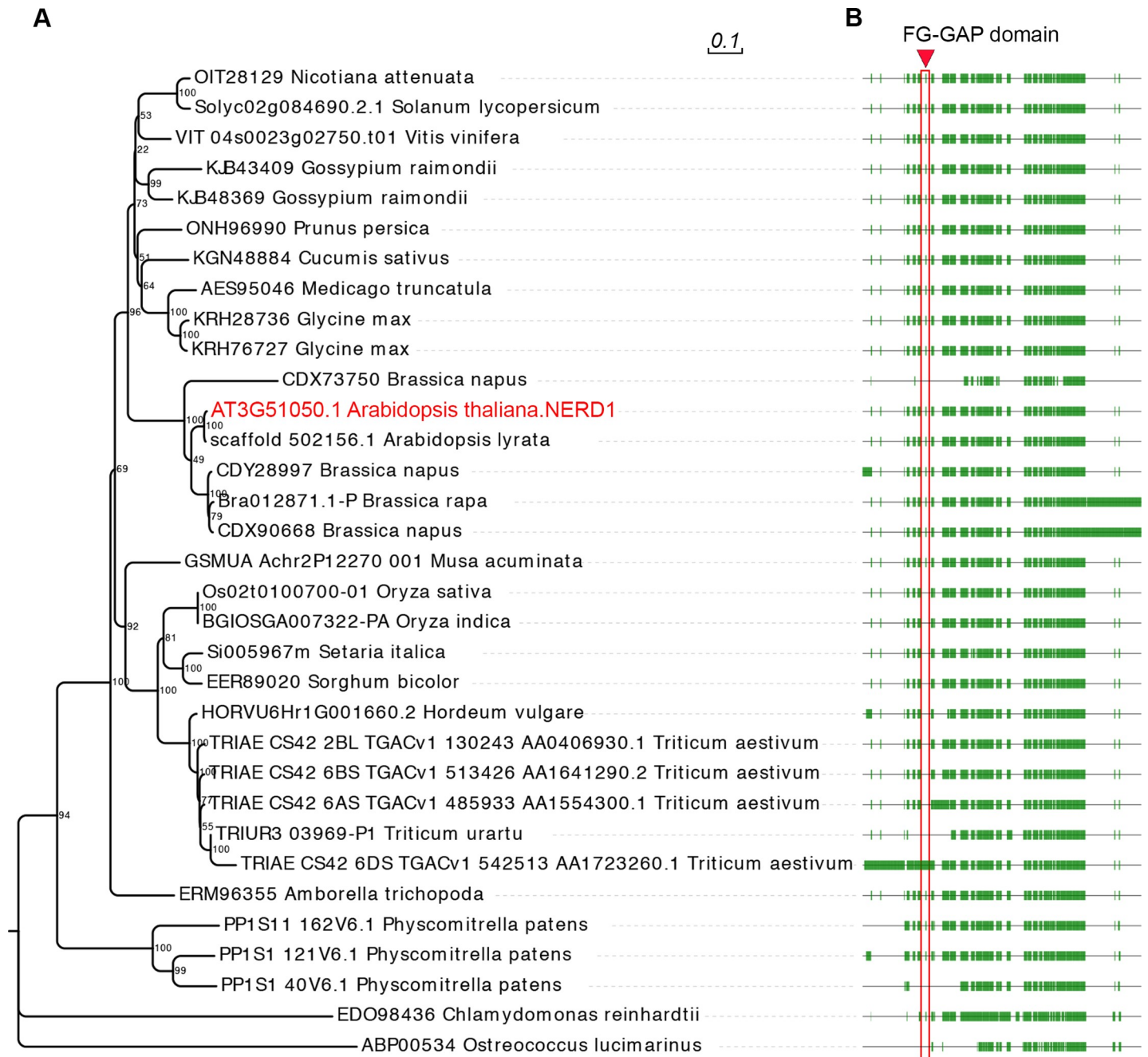


**Fig 4. NERD1 is conserved across plant lineages.** (A) Phylogenetic tree from amino acid alignment of NERD1 generated using the Neighbor-joining method in MEGA7. (B) NERD1 alignment showing sequence conservation among species. The green boxes correspond to conserved regions of NERD1 and the lines represent gaps in the alignment. The red box indicates the FG-GAP domain annotated in NERD1 by Langhans, et al., 2017.

<https://doi.org/10.1371/journal.pgen.1007934.g004>

predicted to be extracellular, with the transmembrane domain located near the C-terminus and a 17 amino acid cytoplasmic extension. Transient expression of a NERD1-GFP fusion in *Nicotiana benthamiana* with subcellular markers confirmed that NERD1 puncta colocalize with the Golgi marker and partially overlap with a plasma membrane marker (Fig 5B and 5D). NERD1 does not co-localize with ER, peroxisome, and plastid markers (Figs 5C and S8). Consistent with NERD1-GFP localization reported in Cole, et al., 2018, our *Arabidopsis* plants

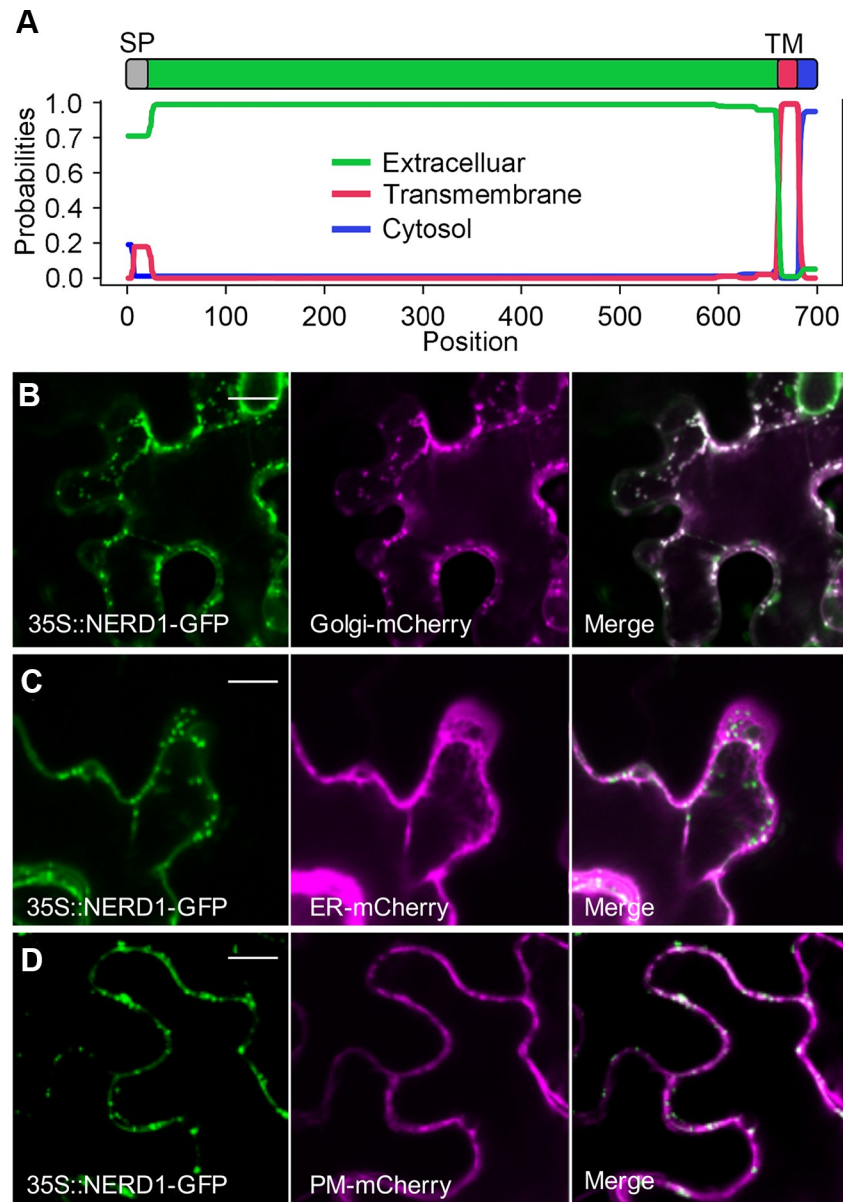


**Fig 5. NERD1 co-localizes with a Golgi marker in *N. benthamiana* epidermal cells.** (A) NERD1 protein domains determined by TMHMM 2.0. (B) NERD1-GFP (green signal) co-localizes with Golgi-mCherry (magenta signal) in *N. benthamiana* epidermal cells. (C) NERD1-GFP (green signal) does not co-localize with ER-mCherry (magenta signal). (D) NERD1-GFP (green signal) partially overlaps with PM-mCherry (magenta signal). Bars = 15  $\mu$ m.

<https://doi.org/10.1371/journal.pgen.1007934.g005>

complemented with the NERD1-tdTomato fusion protein driven by the native NERD1 promoter had NERD1-tdTomato signal in a punctate pattern consistent with Golgi in roots and early stages of ovule development, but it was not detected in plasma membrane (S9 Fig).

### ***NERD1* is expressed throughout Arabidopsis development**

The *nerd1* ovule number and fertility phenotypes suggest that *NERD1* should be expressed in developing flowers. We used a *NERD1*<sub>pro</sub>::*gNERD1-GUS* fusion to examine *NERD1* expression throughout Arabidopsis development. In *NERD1*<sub>pro</sub>::*gNERD1-GUS* inflorescences, GUS

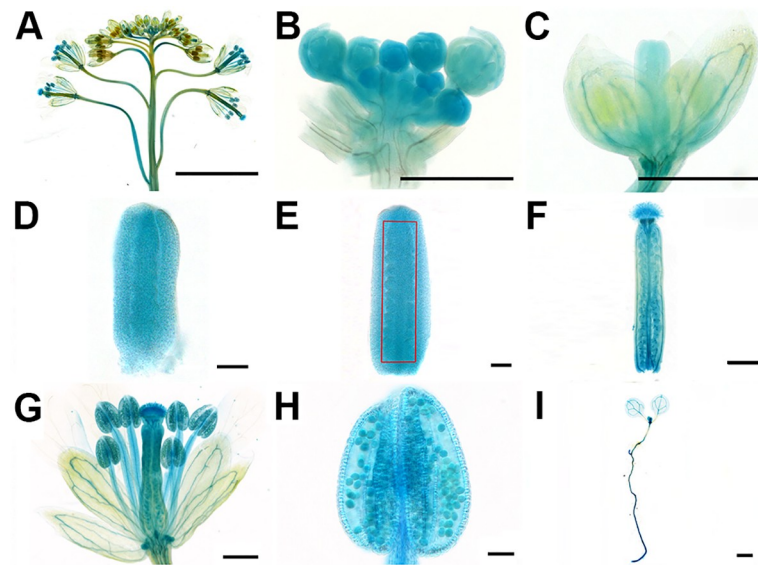


**Fig 6. NERD1 expression in plant development.** The  $NERD1_{pro}::NERD1$ -GUS reporter (blue signal) is detected in inflorescence (A-B), the flower in stage 9 (C), the pistil in stage 8 (D), the pistil in stage 9 (E), mature pistil (F), mature flower (G), mature anther (H), and SAM and RAM of seedlings (I). Bars = 25  $\mu$ m.

<https://doi.org/10.1371/journal.pgen.1007934.g006>

activity was detected throughout flower development, including inflorescences, developing and mature anthers, and in the stigma, ovules, and carpel walls of mature pistils (Fig 6). NERD1-GUS activity was present in the carpel margin meristem (CMM) in stage 9 flowers, where ovule initiation occurs (Fig 6C and 6E). NERD1 reporter expression in the CMM during pistil development is consistent with a role for NERD1 during ovule initiation. During seedling development, the NERD1-GUS reporter was detected in shoot and root apical meristems (SAM and RAM) and in the vasculature (Fig 6I). Our GUS reporter results are consistent with tissue-specific transcriptome data from ePlant (S10 Fig), suggesting that NERD1 is ubiquitously expressed throughout the plant and that the NERD1 promoter used in our experiment accurately reflects endogenous transcription.

### Overexpression of NERD1 increases plant productivity

We examined NERD1 transcript levels in the low ovule number accession Altai-5 compared to Col-0. NERD1 transcript accumulation was reduced in Altai-5 and Kas-2 buds as compared to Col-0 but similar in Altai-5 and Col-0 leaves (Fig 7A and 7B). We hypothesized that the low ovule number in Altai-5 may be linked to reduced NERD1 expression in developing flowers. In order to determine whether increasing NERD1 expression is sufficient to increase ovule number, we transformed Col-0 and the low ovule number accession Altai-5, with a NERD1-GFP fusion construct driven by the constitutively expressed Cauliflower Mosaic Virus 35S promoter (35S::NERD1-GFP). Overexpression of NERD1 had no effect on ovule number in the Col-0 background, but significantly increased ovule number in the Altai-5 background (Fig 8A–8C), indicating that the NERD1 effect on ovule number is background-dependent. The 35S::NERD1-GFP plants displayed an even more striking phenotype when overall plant architecture was examined (Fig 8A). In both the Altai-5 and Col-0 backgrounds, NERD1 overexpression led to increased branching (Fig 8D) and shortened internode lengths between flowers, leading to an overall increase in flower number in the overexpression plants compared to untransformed controls (Fig 8E–8H). Thus, NERD1 overexpression leads to increased biomass and

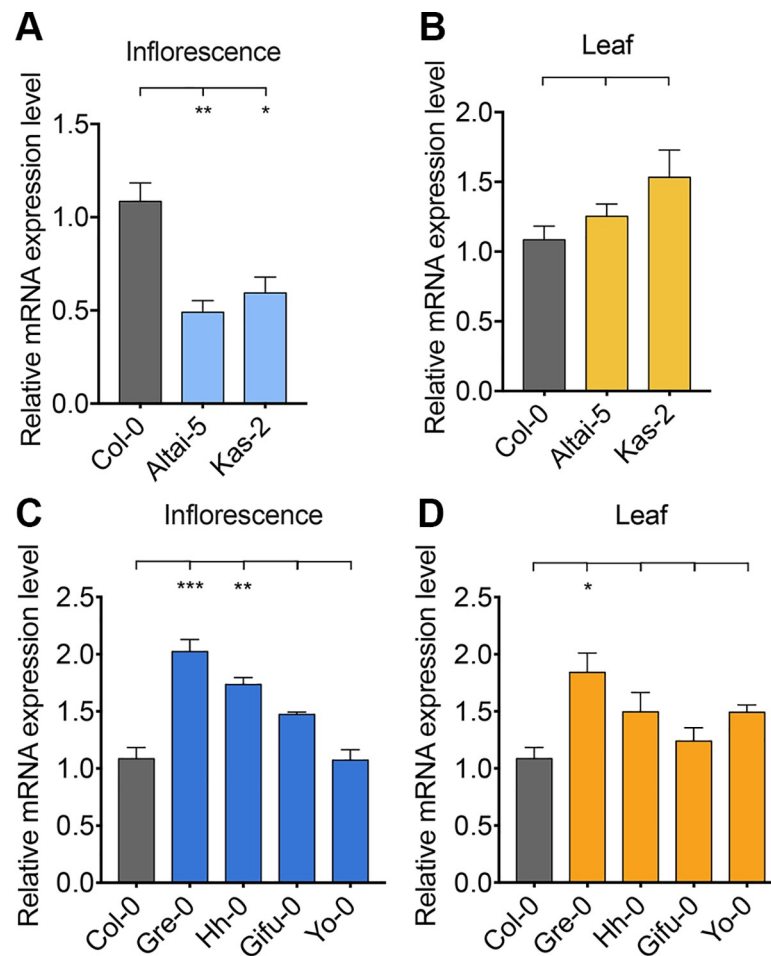


**Fig 7. NERD1 expression is reduced in developing flowers of some specific low ovule number accessions.** (A) qRT-PCR of NERD1 in Col-0, Altai-5 and Kas-2 inflorescences. (B) qRT-PCR of NERD1 in Col-0, Altai-5 and Kas-2 leaves. (C) qRT-PCR of NERD1 in Col-0, Gre-0, Hh-0, Gifu-0 and Yo-0 inflorescences. (D) qRT-PCR of NERD1 in Col-0, Gre-0, Hh-0, Gifu-0 and Yo-0 leaves. “\*\*\*” indicates statistical significance at  $p$  value < 0.001, “\*\*” indicates statistical significance at  $p$  value < 0.01, “\*” indicates statistical significance at  $p$  value < 0.05 determined by Student’s  $t$ -test.

<https://doi.org/10.1371/journal.pgen.1007934.g007>

reproductive capacity, with up to a 2.5-fold increase in total flower number over the lifespan of the plant. While all independent transformants displayed increased branching and flower number, some of the *35S::NERD1* plants were male sterile (S11 Fig). This male sterility correlated with *NERD1* expression levels and plants with higher *NERD1* transcript levels had more severe male sterility (S11 Fig). The sterility effect was more severe in Col-0 than in Altai-5 (S11 Fig). The lower endogenous *NERD1* expression in Altai-5 inflorescences might explain the lower sensitivity of Altai-5 to *NERD1* overexpression with respect to male fertility, demonstrating background-dependent sensitivity to *NERD1* levels for both ovule number and male sterility.

*NERD1* was recently identified in enhancer screen performed on exocyst mutants with weakly dwarfed roots. *nerd1* mutants have reduced root growth as a result of impaired cell expansion, indicating that *NERD1* may be a positive regulator of exocyst-dependent root growth[25]. Consistently, the *35S::NERD1-GFP* plants had longer roots compared to the Col-0 control, indicating that root development is also sensitive to *NERD1* expression levels (S12 Fig).

Four SNPs in *NERD1* exons showed significant correlation with ovule number in our GWAS (Fig 9A and 9B). Three of them are synonymous SNPs that are not predicted to change

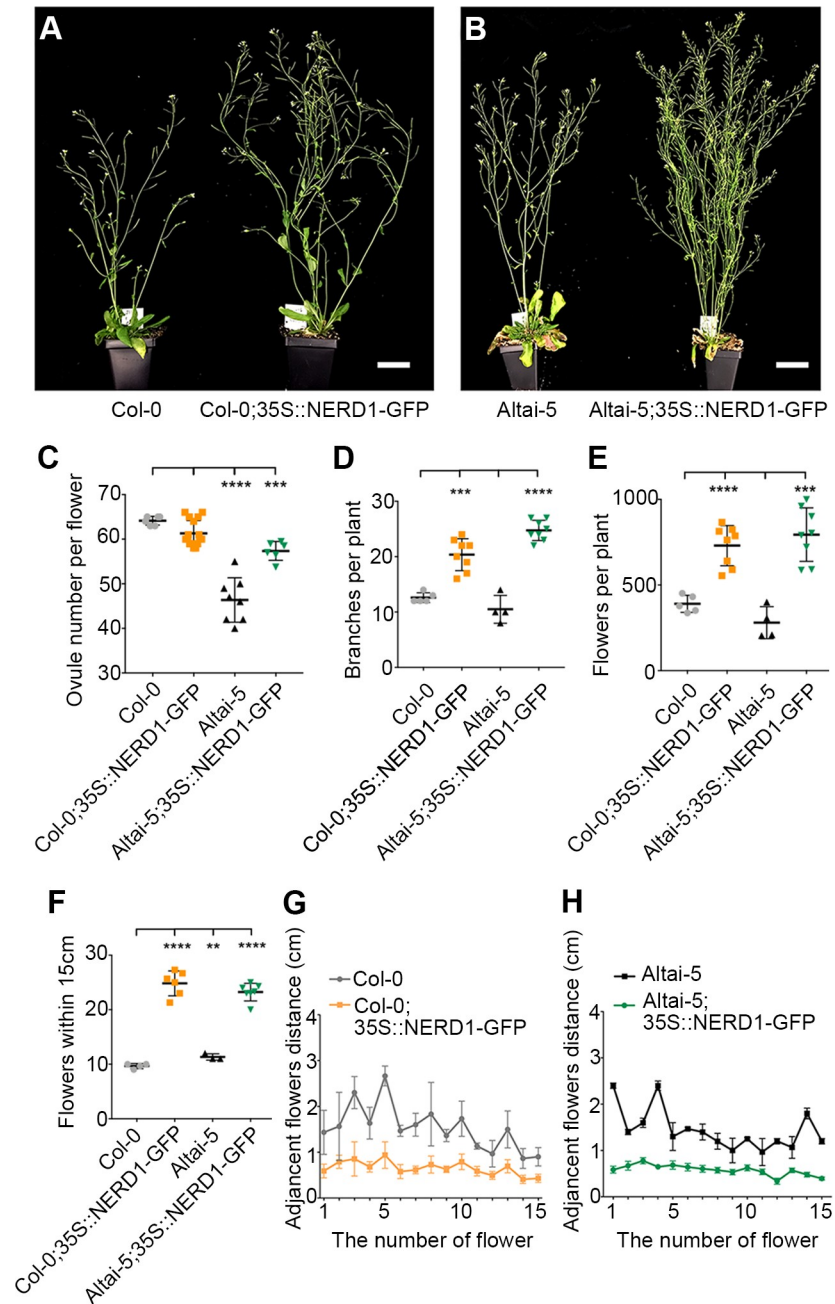


**Fig 8. Overexpression of NERD1 affects plant architecture and fertility.** (A-B) 35S::NERD1-GFP expressed in Col-0 and Altai-5 backgrounds. Bars = 5cm. Scatter plots of total ovule number per flower (C), total branch number (D), total flower number per plant (E), number of flowers within 15 cm of the main shoot (F), and distance between adjacent flowers (G-H) in 35S::NERD1-GFP transformants in the Col-0 and Altai-5 backgrounds compared to untransformed controls.

<https://doi.org/10.1371/journal.pgen.1007934.g008>

the amino acid sequence, but the fourth is a non-synonymous SNP (C to A change in comparison to Col-0 reference) causing a Serine to Tyrosine change at amino acid 230 of NERD1 (Fig 9A and 9B). This non-synonymous SNP was present in 10 out of the 16 lowest ovule number accessions and not present in the 16 highest ovule number accessions (Fig 9A). Across all of the accessions in our GWAS panel, the “A” allele at this position was significantly associated

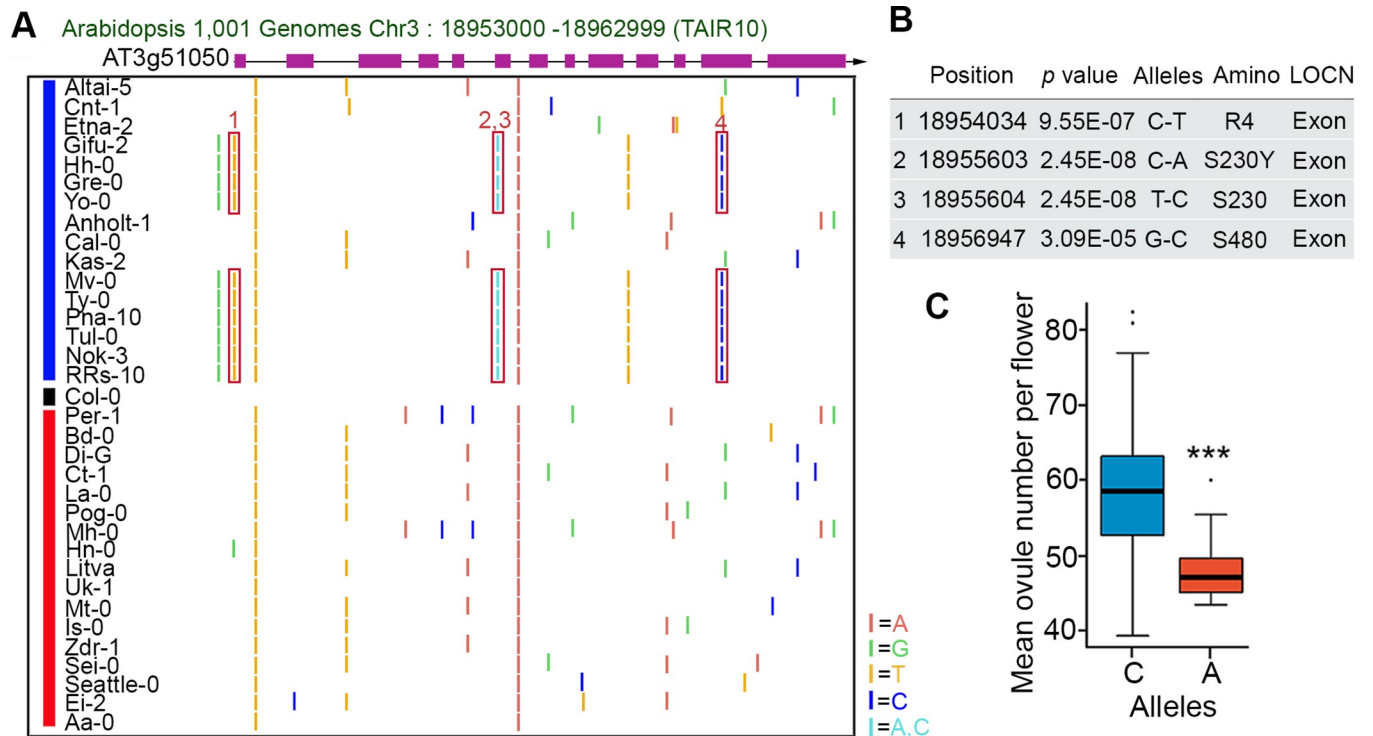


**Fig 9. Sequence variation in the *NERD1* locus correlates with ovule number.** (A) SNPs in and around the *NERD1* gene. The blue line indicates the 16 lowest ovule number accessions and the red line indicates the 16 highest ovule number accessions. SNPs are identified based on comparison to the Col-0 reference genome. The red boxes highlight low-ovule number associated SNPs (the turquoise bar indicates two SNPs in adjacent nucleotides, a non-synonymous C-A SNP and a synonymous C-G SNP). Only genomes that were available on the SALK 1,001 genomes browser (<http://signal.salk.edu/atg1001/3.0/gebrowser.php>) were considered. (B) One of the ovule number-associated SNPs in *NERD1* causes a serine-tyrosine substitution in low ovule number accessions. (C) Average ovule number in *NERD1* “A” and “C” allele-containing accessions. The “A” allele is significantly associated with lower ovule numbers. “\*\*\*” indicates statistical significance at  $p$  value < 0.001 determined by Student’s t-test.

<https://doi.org/10.1371/journal.pgen.1007934.g009>

with lower ovule numbers (Fig 9C). However, some accessions with the “C” allele of *NERD1* have low ovule numbers (Fig 9A), including the Altai-5 accession described above. We examined *NERD1* transcript levels in additional low ovule number accessions to determine if *NERD1* expression correlated with ovule number in other accessions. Like Altai-5, the “C” allele accession Kas-1 had reduced *NERD1* transcript levels in flowers when compared to Col-0 (Fig 7A and 7B). However, four “A”-containing accessions with the S230Y amino acid change had similar or higher expression levels of *NERD1* in developing flowers (Fig 7C and 7D), indicating that reduced *NERD1* expression in flowers is not the explanation for reduced ovule number in these accessions. A second possibility is that the S230Y amino acid change affects the protein function of *NERD1* in these accessions. To test this hypothesis, we transformed *nerd1-2* mutants with *NERD1* from both Gre-0 and Hh-0 expressed as td-Tomato fusions driven by their native promoters. Both of these *NERD1* genes could complement the *nerd1-2* ovule number phenotype (S13 Fig), indicating that some other mechanism influences ovule number in these accessions.

## Discussion

Our experiments revealed that Arabidopsis displays a wide variation in the number of ovules per flower, a key component of plant fitness and crop yield. Association genetics linked this natural variation to the plant-specific gene, *NERD1*, that regulates the number of ovules

produced in *Arabidopsis* flowers and gametophyte development (Fig 3) and was previously found to alter root growth[25]. Overexpression of *NERD1* led to dramatic effects on plant architecture, indicating that *NERD1* may be involved in regulating meristem activity during *Arabidopsis* development.

### GWAS reveals new ovule number-associated loci in *Arabidopsis*

A quantitative trait locus (QTL) mapping study utilizing variation between *Ler* and *Cvi* identified QTL residing on chromosomes 1, 2 (near the *ERECTA* gene), and two QTL on chromosome 5[23]. No follow-up study has identified the genes underlying these QTL. Our population displayed a much larger range of ovule numbers per flower (39–84) than that seen in *Cvi* vs *Ler* (66 and 56, respectively). We identified 9 significant associations in our GWAS, but only one potentially overlaps with a known ovule number QTL (see chromosome 5 in S2 Fig). Of the genes with an identified effect on ovule number, only *BIN2* overlapped with a GWAS peak, indicating that our study has revealed at least seven novel regulators of ovule number in *Arabidopsis*. We molecularly identified two new genes that control ovule number that were linked to two GWAS peaks on chromosome 3. This expands that number of known ovule number determinants and confirms the value of GWAS as a forward genetics tool.

### *NERD1* may play a role in the secretory system

*NERD1* is a plant-specific, low copy number gene that is found throughout the plant kingdom. *NERD1* was recently identified as an enhancer of root development phenotypes in weak mutants of the exocyst subunits *SEC8* and *EXO70A1*[25]. While a direct interaction with the exocyst could not be identified, the authors identified Golgi localization of *NERD1* and hypothesized that *NERD1* could be involved in synthesizing or modifying pectins or other polysaccharide components of the cell wall that are synthesized in the Golgi and transported to the cell wall [25]. Changes in cell wall elasticity mediated by pectin modifications have been correlated with lateral organ initiation at the shoot apical meristem [28, 29]. The decreased ovule number in *nerd1* mutants and increased lateral branching and flower initiation in 35S::*NERD1* transformants could be consistent with alterations in Golgi-synthesized cell wall components affecting cell wall mechanics and organ initiation.

### *NERD1* and fertility

Homozygous *nerd1* mutants are completely male sterile and partially female sterile. This sterility is due to a lack of pollen production and problems in female gametophyte development leading to aborted embryo sacs. Transmission efficiency tests using heterozygous loss-of-function mutants revealed that *nerd1* could be transmitted through the egg at near 100% efficiency, indicating a sporophytic effect on female gametophyte development. Ovule development mutants that have defective integument development such as *short integuments 1* (*sin1*), *bell 1* (*bell1*) and *ant* fail to produce functional female gametophytes, indicating that female gametophyte development is dependent on properly differentiated sporophytic cells in the ovule[30–34]. Sporophytic development in ovules seem to be normal in *nerd1* mutants, yet embryo sacs abort. As a membrane protein, *NERD1* could transmit some unknown signal between sporophytic and gametophytic cells during embryo sac development.

The male fertility defect in *nerd1* plants is more severe than the female defect. Homozygous *nerd1* anthers have severe reductions in pollen production resulting from defects in early stages of pollen development. Transmission efficiency tests using pollen from heterozygous *nerd1* plants crossed to wild-type females revealed that *nerd1* also has gametophytic effects on pollen function. The sporophytic effects could be related to early stages of anther development.

In particular, specification of the tapetum is critical for pollen development (reviewed in [35]). In our 35S::*NERD1* experiment, transformants that accumulated the most *NERD1* transcripts were male sterile. Together these results indicate that pollen development is sensitive to *NERD1* levels, i.e. either too much or too little *NERD1* is detrimental to pollen development. Future experiments should focus on determining the stage of anther and/or pollen development that is affected in *nerd1* mutants and the specific cell types that express *NERD1* in developing anthers.

Even though *NERD1* is expressed broadly throughout the plant, above ground vegetative development appears to be normal in *nerd1* loss-of-function mutants. However, *nerd1* roots are shorter than normal and have root hair defects that include bulging and rupture [25]. *NERD1* could have distinct or related developmental functions in roots and flowers, as is seen for many of the genes involved in hormonal regulation of development [36].

### ***NERD1* and lateral organ formation**

*NERD1* overexpression under control of the constitutive 35S promoter dramatically changed plant architecture in both the Col-0 and Altai-5 backgrounds. Overexpression phenotypes can be difficult to interpret since the 35S promoter could be active in cells where *NERD1* is not normally expressed, causing *NERD1* to interfere with pathways specific to those cell types. Alternatively, the increase in lateral organ formation seen in 35S::*NERD1* plants could be related to increased root capacity that changes source/sink relationships within the plant and leads to higher plant productivity. This hypothesis is consistent with the smaller roots reported in *nerd1* mutants and could be related to the secretory machinery and trafficking [25]. A third possibility is that *NERD1* is a positive regulator of meristem activity. *NERD1* overexpression plants produced significantly more branches than wild-type controls and produced significantly more flowers that were produced at closer intervals along the stem. Like branches and flowers, ovules are lateral organs produced from meristematic cells. Lateral meristem activation and subsequent branching have been shown to be affected by several different hormones (reviewed in [37]). Classic experiments in *Vicia faba* showed that auxin produced in the shoot apex inhibits axillary meristems [38], and more recently strigolactones were identified as graft-transmissible suppressors of branching (reviewed in [39]). Gibberellins also repress shoot branching in *Arabidopsis*, maize, and rice, with GA-deficient mutants displaying increased branching compared to wild-type controls [40–43]. In contrast, cytokinins and brassinosteroids are both positive regulators of branching [42–46]. The mechanism through which these plant hormones work together to regulate branching is unknown, but auxin has been proposed to control cytokinin and strigolactone biosynthesis [47, 48], while the brassinosteroid signaling regulator *BES1* may inhibit strigolactone signaling to promote branching [49]. The promotion of branching in 35S::*NERD1* plants could be related to regulation of one or more of these hormonal pathways. Like *NERD1*, upregulation of both cytokinin and brassinosteroid signaling pathways have been shown to positively regulate branching and ovule number [15, 46, 49, 50], suggesting that *NERD1* may be intimately connected to these pathways. Future research is needed to explore the intersection between *NERD1* and hormonal pathways.

### ***NERD1*-induced increases in ovule number are background-dependent**

Overexpression of *NERD1* in the Col-0 and Altai-5 backgrounds led to increased branching and flower number, but ovule number was only increased in the Altai-5 background, suggesting a background-dependence on the ovule number trait. In *Arabidopsis*, natural accessions were shown to respond differently in their ability to buffer GA perturbations caused by overexpressing GA20 oxidase 1, which encodes a rate-limiting enzyme for GA biosynthesis [51].

Genetic background dependence has been shown to be a wide-spread phenomenon in *C. elegans*, with approximately 20% of RNAi-induced mutations (out of 1400 genes tested) displaying different phenotypic severity in two different genetic backgrounds[52]. Similar to our results with *NERD1*, where Altai-5 has lower endogenous levels of the *NERD1* transcript in developing flowers compared to Col-0, the severity of the *C. elegans* phenotypes could be linked to gene expression levels of either the target gene itself or other genes in the same pathway[52].

Our GWAS revealed multiple novel loci that control ovule number in *Arabidopsis*. It remains to be seen if exocyst function is linked to *NERD1*'s role in ovule number determination. Identification of *NERD1* interacting proteins will provide candidates for other players in the *NERD1* pathway. Some of the other novel loci identified in our GWAS may well participate in the same signaling pathway as *NERD1*. While *NERD1* is a promising candidate for engineering plants with increased ovule number, the differential responses to *NERD1* overexpression seen in Altai-5 and Col-0 suggest that specific alleles at other loci may be necessary for achieving maximum effect of *NERD1* overexpression.

## Materials and methods

### Plant material and growth conditions

*Arabidopsis thaliana* accessions and insertion mutants were ordered from the Arabidopsis Biological Resource Center at Ohio State University (ABRC). ABRC stock numbers for the accessions and insertion mutants used in our study are listed in S1 and S2 Tables. Seeds were sterilized and plated on ½ Murashige and Skoog (MS) plates. All plates were sealed and stratified at 4°C for two days, and then transferred to the growth chamber (long day conditions, 16h of light and 8 h of dark at 22°C) for germination and growth. After one-week, seedlings were transplanted to soil. Many of the *Arabidopsis* accessions require vernalization for flowering [53], we therefore chose to vernalize all of the accessions in our study for 4 weeks at 4°C. After vernalization, the plants were returned to the growth chamber and grown under the long day conditions described above. Seeds from transformed lines were sterilized and plated on ½ MS plate with 20mg/L hygromycin for selection of transgenic seedlings, which were then transplanted to soil and grown in long days.

### Ovule number phenotyping

For determination of ovule number per flower, we counted four to five siliques per plant and five plants per accession. Carpel walls were removed with a dissecting needle and total ovule number (including unfertilized and aborted ovules) was counted with the aid of a Leica dissecting microscope. To minimize age-related variation in ovule number, we counted siliques from flowers 6–10 on the primary shoot for all accessions.

### Genome-Wide association study

GWAS was performed using GWAPP, which is a GWAS web application for Genome-Wide Association Mapping in *Arabidopsis* (<http://gwas.gmi.oeaw.ac.at>) [22]. In our study, 148 accessions had single nucleotide polymorphisms (SNPs) data available on the 1001 Full-sequence dataset; TAIR 9. Logarithmic transformation was applied to make the results more reliable for parametric tests. A simple linear regression (LM) was used to generate the Manhattan plot by using GWAPP[22]. SNPs with P values  $\leq 1 \times 10^{-6}$  were further considered as candidate loci linked to alleles that regulate ovule number (a horizontal dashed line in Fig 2 shows the 5% FDR threshold  $-\log_{10}p$  value = 6.2, which was computed by the Benjamini-Hochberg-Yekutieli

method). SNPs with < 15 minor allele count (MAC) were not considered to help control false positive rates. 10 genes flanking the highest SNP for each locus were tabulated as candidate genes for each significant association.

### Cloning and generation of transgenic lines

For complementation and overexpression experiments, Gateway Technology was used to make all the constructs. Genomic DNA fragments corresponding to the coding regions of candidate genes were amplified from either beginning of the promoter (defined by the end of the upstream gene) or the start codon to the end of the CDS (without stop codon) by PCR with primers that had attB1 and attB2 sites from Col-0 genomic DNA (see S3 Table for primer sequences). For amplifying At3g60660 and At3g51050, PHUSION High-Fidelity Polymerase (NEB, M0535S) was used. All the PCR products were put into entry vector pDONR207 by BP reactions and then were recombined into destination vector pMDC83 (GFP) by LR reaction [54]. Native promoter constructs were amplified from ~2KB promoter region to the end (without stop codon) by PCR with primers that had attB1 and attB2 sites from Col-0 genomic DNA. The PCR products were put into entry vector pDONR207 by BP reactions and then were recombined into destination vector pMDC32 (tdTomato) and pMDC163 (GUS) by LR reaction. All constructs were transformed into *Agrobacterium tumefaciens* strain GV3101 and then used for plant transformation by the floral-dip method[55].

### GUS staining

GUS staining was performed as previously described[56]. Samples were imaged with Differential Interference Contrast (DIC) on a Nikon Eclipse Ti2-E microscope. 12 independent T1 NERD-GUS transformants were analyzed and showed similar GUS patterns.

### Transient expression in *N. benthamiana*

Leaves from 3–4 week old *N. benthamiana* were co-infiltrated with 35S::NERD1-GFP and Golgi-mCherry, ER-mCherry, PM-mCherry, Plastid-mCherry and Peroxisome-mCherry markers from[57] as previously described[58]. Leaves were imaged 2–3 days after infiltration with a Nikon A1Rsi inverted confocal microscope under 20x dry and 40x water objectives with GFP excited by a 488nm laser and mCherry excited by a 561nm laser in normal mode.

### Analysis of embryo sac and pollen development

Analysis of embryo sac development was conducted using confocal microscopy based on [59]. Pistils were dissected from FG2, FG3, FG4 and mature stages of flowers from Col-0, *nerd1-2* and *nerd1-4* and fixed in 4% glutaraldehyde and 12.5mM cacodylate, PH = 6.9 for two hours at room temperature. Pistils were dehydrated in 20%, 40%, 60%, 80% and 100% ethanol for 10 min each. Samples were then cleared in a 2:1 mixture of benzyl benzonate: benzyl alcohol for 2–4 hours and mounted in immersion oil for imaging. Images were captures using a Nikon A1Rsi inverted confocal microscope under 60x oil objectives and excitation with a 561 nm laser.

Pollen was released from tetrad, microspore, bi-cellular, tri-cellular and mature stage anthers from Col-0, *nerd1-2* and *nerd1-4*. Samples were incubated in 1ug/ml DAPI (4',6-diamidino-2-phenylindole) staining solution for 2hrs and imaged using a Nikon A1Rsi inverted confocal microscope under 60x oil objectives with DAPI excited by a 405nm laser.

### Alexander staining of mature pollen

Mature anthers from Col-0 and *nerd1-2/nerd1-2* were dissected under the Leica dissecting microscope and placed into a drop (20  $\mu$ l) of Alexander staining solution on a microscope slide[60]. After several minutes of staining, samples were imaged with a Nikon Eclipse Ti2-E microscope.

### Aniline blue staining of pollen tube behavior

Flowers that two days after emasculation from *nerd1-2* plants were cross-pollinated with wild-type Col-0. The pollinated pistils were then collected at 36 h after hand pollination and fixed immediately in ethanol-acetic acid (3:1 v/v) overnight. Pistils were rehydrated in 70%, 50%, 30% ethanol for 5 min each at room temperature. After clearing in 5 N NaOH at 60°C for 5 min and washing 2  $\times$  in 0.1M phosphate buffer (pH-8), they were stained using aniline blue (0.1% aniline blue in K<sub>3</sub>PO<sub>4</sub>) for 15mins. Five pistils per sample were analyzed and images were captured with a Nikon Eclipse Ti2-E microscope (Nikon Instruments Inc, Melville, NY).

### Phylogenetic analysis

The cladogram tree was generated in MEGA7, which nucleotide distance and neighbor-join tree file were calculated by PHYlogeny Inference Package (PHYMLIP, version 3.696).

The phylogenetic tree of NERD1 was inferred using neighbor-joining method in MEGA7 [61]. The associated taxa clustered together with the bootstrap test (1000 replicates)[62]. All the branch lengths are in the same units as those of the evolutionary distances used to generate the phylogenetic tree.

### Quantitative real-time RT-PCR

For qRT-PCR, leaves and young flowers were collected from mature plants of Col-0 and Altai-5. Samples were immediately frozen in liquid nitrogen, ground, and total RNA was extracted using the E.Z.N.A Plant RNA kit (OMEGA, USA). Oligo-dT primers and Superscript II reverse transcriptase (Invitrogen) was used for cDNA synthesis. qRT-PCR reactions were prepared using SYBR Green PCR Master Mix and PCR was conducted with a StepOnePlus RT-PCR system. Relative quantifications were performed for all genes with the Actin11 used as an internal reference. The primers used for qRT-PCR shown in S3 Table.

### Supporting information

**S1 Fig. Statistical analysis of the relationship between ovule number per flower and geographical origin of the accessions used in the GWAS.** (A-B) A weakly positive correlation was detected between latitude and ovule number when all accessions were considered. (C-D) No correlation between ovule number and latitude or longitude was identified when only European accessions were tested. A Pearson correlation coefficient was computed to assess the relationship between the ovule number per flower and their geographic distribution of latitude or longitude, respectively. There was a slight correlation between the ovule number per flower and latitude distribution when accessions from all locations were tested [ $r^2 = 0.0289$ ,  $p$  value = 0.034]. There was no correlation between the ovule number per flower and longitude when accessions from all locations were tested [ $r^2 = 0.0006$ ,  $p$  value = 0.757]. There was no correlation between the ovule number per flower and latitude or longitude of the accessions' origin when only European accessions were tested [ $r^2 = 0.0001$  or 0.0005,  $p$  value = 0.899 or 0.813], respectively.

(PDF)

**S2 Fig. Previously identified ovule number related genes' positions in relation to the Manhattan plot from the ovule number GWAS.** The Manhattan plot is the same as in Fig 2. Red lines indicate the known ovule number related genes. Blue boxes indicate the genomic regions underlying 4 ovule number QTL identified by [23].  
(PDF)

**S3 Fig. Heat map of candidate gene expression patterns in reproductive tissues.** Colors from blue to red indicate the gene expression level from low to high.  
(PDF)

**S4 Fig. Total ovule number per flower of all available T-DNA insertion mutants in ovule number-associated genomic regions on chromosome 3.** “\*\*\*\*” indicates statistical significance ( $p$  value < 0.0001 determined by Student's t-test).  
(PDF)

**S5 Fig. Pollen tube guidance in *nerd1-2* mutants.** (A) Homozygous *nerd1* mutants have high levels of infertility that can be partially rescued by pollinating with Col-0 wild-type pollen. (B) Aniline blue staining for *nerd1-2/nerd1-2* pollinated with Col-0 pollen. Arrows indicate fertilized ovules with normal pollen tube attraction and stars indicate unfertilized ovules without pollen tube attraction. Bar = 100  $\mu$ m. (C) Quantification of pollen tube attraction percentage for *nerd1-2/nerd1-2* plants pollinated with Col-0 pollen (black indicates fertilized ovules with pollen tubes and gray indicates unfertilized ovules with no pollen tubes). 5 pistils were analyzed for each cross.  
(PDF)

**S6 Fig. *nerd1-2* has both male and female defects.** (A) Examples of defective embryo sacs in *nerd1-2/nerd1-2* mature ovules. Bar = 50  $\mu$ m. (B) In comparison to Col-0, *nerd1-2/nerd1-2* has defective microspores and an absence of later pollen stages. Bar = 15  $\mu$ m.  
(PDF)

**S7 Fig. *nerd1-4* has defective embryo sacs and reduced pollen production.** (A) Aborted embryo sac in a mature *nerd1-4* ovule. Bar = 50  $\mu$ m. (B) Comparison of normal (black) vs. defective (gray) embryo sac percentages in Col-0 and *nerd1-4* pistils. (C) Fewer viable pollen grains are present in Alexander stained anthers of *nerd1-4/nerd1-4* compared to Col-0. Bar = 100  $\mu$ m. (D) T-DNA insertion sites in the NERD1 gene (boxes indicate exons and lines indicate introns).  
(PDF)

**S8 Fig. Co-localization of 35S::NERD1-GFP with subcellular markers.** (a) 35S::NERD1-GFP (green signal) does not co-localize with Peroxisome-mCherry and (b) Plastid-mCherry (magenta) markers in *N. benthamiana* epidermal cells. Scale bar = 25  $\mu$ m.  
(PDF)

**S9 Fig. NERD1 localization in Arabidopsis transgenic lines expressing pNERD1::NERD1-TdTomato.** (A) NERD1-TdTomato is present in a punctate compartment in root epidermal cells. (B) NERD1 localization in ovules at flower developmental stages 9, 10 and 11. (C) Magnification of stage 11 from panel B showing punctate NERD1 accumulation in the nucellus around the megaspore mother cell (dashed circle). Bars = 30  $\mu$ m (A), 20  $\mu$ m (B), 10  $\mu$ m (C).  
(PDF)

**S10 Fig. NERD1 is constitutively expressed throughout Arabidopsis development.** (A) NERD1 expression level in different tissues from publicly available transcriptome data in

ePlant. (B)  $NERD1_{pro::g}$ NERD1-GUS fusion construct data (see Fig 6) matches the ePlant transcriptome data.  
(PDF)

**S11 Fig. 35S::NERD1 plants have variable fertility.** (a) The number of sterile plants and normal T1 plants in Col-0 and Altai-5. (b) qRT-PCR of NERD1 in 35S::NERD1 plants in Col-0 background. Yellow bars represent plants with normal fertility and blue bars indicate male sterile plants.  
(PDF)

**S12 Fig. NERD1 is involved in root growth.** (a) Root phenotype in Col-0, *nerd1-2/nerd1-2*, 35S::NERD1, and the NERD1 complementation line. *nerd1* mutants have significantly shorter roots while overexpression of NERD1 leads to longer roots than the Col-0 control. Bar = 0.7 cm. (b) Bar graph of the quantification of the root length. “\*\*\*\*” indicates statistical significance ( $p$  value < 0.0001 determined by Student’s t-test). “\*\*\*\*” indicates statistical significance ( $p$  value < 0.001 determined by Student’s t-test,  $n$  = at least 9 individuals for each genotype).  
(PDF)

**S13 Fig. *nerd1-2* reduced ovule number phenotype can be rescued by NERD1 complementation constructs derived from Col-0, Gre-0 and Hh-0.** ( $p$  value < 0.0001 determined by Student’s t-test).  
(PDF)

**S1 Table. List of Arabidopsis accessions used in the study and their ovule number data.**  
(XLSX)

**S2 Table. Chromosome 3 candidate genes and insertion mutants.**  
(XLSX)

**S3 Table. List of primers used for genotyping and cloning.**  
(XLSX)

## Acknowledgments

We thank Dr. Brian Dilkes, Dr. Leonor Boavida, Dr. John Fowler, Dr. Daniel S. Jones, Dr. Yan Ju, Thomas Davis, and Rachel Flynn for helpful discussions and comments on the manuscript. We thank Dr. Xutong Wang for help with the statistical analysis.

## Author Contributions

**Conceptualization:** Jing Yuan, Sharon A. Kessler.

**Data curation:** Jing Yuan.

**Formal analysis:** Jing Yuan, Sharon A. Kessler.

**Funding acquisition:** Sharon A. Kessler.

**Investigation:** Jing Yuan.

**Methodology:** Jing Yuan.

**Project administration:** Jing Yuan, Sharon A. Kessler.

**Resources:** Sharon A. Kessler.

**Supervision:** Sharon A. Kessler.

**Validation:** Jing Yuan.

**Visualization:** Jing Yuan.

**Writing – original draft:** Jing Yuan.

**Writing – review & editing:** Jing Yuan, Sharon A. Kessler.

## References

- Palmer RG, Albertsen MC, Heer H. Pollen production in soybeans with respect to genotype, environment, and stamen position. *Euphytica*. 1978; 27(2):427–33. <https://doi.org/10.1007/bf00043168>
- Uribelarrea M, Cárcova J, Otegui ME, Westgate ME. Pollen Production, Pollination Dynamics, and Kernel Set in Maize. *Crop Science*. 2002; 42:1910–8. <https://doi.org/10.2135/cropsci2002.1910>
- Yan J, Chia JC, Sheng H, Jung HI, Zavodna TO, Zhang L, et al. Arabidopsis Pollen Fertility Requires the Transcription Factors CITF1 and SPL7 That Regulate Copper Delivery to Anthers and Jasmonic Acid Synthesis. *Plant Cell*. 2017; 29(12):3012–29. Epub 2017/11/09. <https://doi.org/10.1105/tpc.17.00363> PMID: 29114014; PubMed Central PMCID: PMC5757271.
- Coen ES, Meyerowitz EM. The war of the whorls: genetic interactions controlling flower development. *Nature*. 1991; 353(6339):31–7. Epub 1991/09/05. <https://doi.org/10.1038/353031a0> PMID: 1715520.
- Smyth DR, Bowman JL, Meyerowitz EM. Early flower development in Arabidopsis. *Plant Cell*. 1990; 2(8):755–67. Epub 1990/08/01. <https://doi.org/10.1105/tpc.2.8.755> PMID: 2152125; PubMed Central PMCID: PMC159928.
- Reyes-Olalde JI, Zuniga-Mayo VM, Chavez Montes RA, Marsch-Martinez N, de Folter S. Inside the gynoecium: at the carpel margin. *Trends Plant Sci*. 2013; 18(11):644–55. Epub 2013/09/07. <https://doi.org/10.1016/j.tplants.2013.08.002> PMID: 24008116.
- Robinson-Beers K, Pruitt RE, Gasser CS. Ovule Development in Wild-Type Arabidopsis and Two Female-Sterile Mutants. *Plant Cell*. 1992; 4(10):1237–49. Epub 1992/10/01. <https://doi.org/10.1105/tpc.4.10.1237> PMID: 12297633; PubMed Central PMCID: PMC5757271.
- Drews GN, Koltunow AM. The female gametophyte. *Arabidopsis Book*. 2011; 9:e0155. Epub 2012/02/04. <https://doi.org/10.1199/tab.0155> PMID: 22303279; PubMed Central PMCID: PMC3268550.
- Cucinotta M, Colombo L, Roig-Villanova I. Ovule development, a new model for lateral organ formation. *Front Plant Sci*. 2014; 5:117. Epub 2014/04/12. <https://doi.org/10.3389/fpls.2014.00117> PMID: 24723934; PubMed Central PMCID: PMC3973900.
- Klucher KM, Chow H, Reiser L, Fischer RL. The AINTEGUMENTA gene of Arabidopsis required for ovule and female gametophyte development is related to the floral homeotic gene APETALA2. *Plant Cell*. 1996; 8(2):137–53. <https://doi.org/10.1105/tpc.8.2.137> PMID: 8742706.
- Azhakanandam S, Nole-Wilson S, Bao F, Franks RG. SEUSS and AINTEGUMENTA mediate patterning and ovule initiation during gynoecium medial domain development. *Plant Physiol*. 2008; 146(3):1165–81. WOS:000256412200041. <https://doi.org/10.1104/pp.107.114751> PMID: 18184731
- Galbiati F, Sinha Roy D, Simonini S, Cucinotta M, Ceccato L, Cuesta C, et al. An integrative model of the control of ovule primordia formation. *Plant J*. 2013; 76(3):446–55. Epub 2013/08/15. <https://doi.org/10.1111/tbj.12309> PMID: 23941199.
- Nemhauser JL, Feldman LJ, Zambryski PC. Auxin and ETTIN in Arabidopsis gynoecium morphogenesis. *Development*. 2000; 127(18):3877–88. PMID: 10952886.
- Bencivenga S, Simonini S, Benkova E, Colombo L. The transcription factors BEL1 and SPL are required for cytokinin and auxin signaling during ovule development in Arabidopsis. *Plant Cell*. 2012; 24(7):2886–97. Epub 2012/07/13. <https://doi.org/10.1105/tpc.112.100164> PMID: 22786869; PubMed Central PMCID: PMC3426121.
- Bartrina I, Otto E, Strnad M, Werner T, Schmulling T. Cytokinin regulates the activity of reproductive meristems, flower organ size, ovule formation, and thus seed yield in Arabidopsis thaliana. *Plant Cell*. 2011; 23(1):69–80. Epub 2011/01/13. <https://doi.org/10.1105/tpc.110.079079> PMID: 21224426; PubMed Central PMCID: PMC3051259.
- Huang HY, Jiang WB, Hu YW, Wu P, Zhu JY, Liang WQ, et al. BR Signal Influences Arabidopsis Ovule and Seed Number through Regulating Related Genes Expression by BZR1. *Molecular Plant*. 2013; 6(2):456–69. WOS:000317006000019. <https://doi.org/10.1093/mp/sss070> PMID: 22914576
- Gomez MD, Barro-Trastoy D, Escoms E, Saura-Sanchez M, Sanchez I, Briones-Moreno A, et al. Gibberellins negatively modulate ovule number in plants. *Development*. 2018; 145(13). Epub 2018/06/20. <https://doi.org/10.1242/dev.163865> PMID: 29914969.

18. Weigel D. Natural variation in *Arabidopsis*: from molecular genetics to ecological genomics. *Plant Physiol.* 2012; 158(1):2–22. Epub 2011/12/08. <https://doi.org/10.1104/pp.111.189845> PMID: 22147517; PubMed Central PMCID: PMC3252104.
19. Atwell S, Huang YS, Vilhjalmsón BJ, Willems G, Horton M, Li Y, et al. Genome-wide association study of 107 phenotypes in *Arabidopsis thaliana* inbred lines. *Nature.* 2010; 465(7298):627–31. Epub 2010/03/26. <https://doi.org/10.1038/nature08800> PMID: 20336072; PubMed Central PMCID: PMC3023908.
20. Wetzsteini HY, Yi WG, Porter JA, Ravid N. Flower Position and Size Impact Ovule Number per Flower, Fruitset, and Fruit Size in Pomegranate. *J Am Soc Hortic Sci.* 2013; 138(3):159–66. WOS:000333230100001.
21. Stinchcombe JR, Weinig C, Ungerer M, Olsen KM, Mays C, Halldorsdóttir SS, et al. A latitudinal cline in flowering time in *Arabidopsis thaliana* modulated by the flowering time gene *FRIGIDA*. *Proc Natl Acad Sci U S A.* 2004; 101(13):4712–7. Epub 2004/04/09. <https://doi.org/10.1073/pnas.0306401101> PMID: 15070783; PubMed Central PMCID: PMC384812.
22. Seren U, Vilhjalmsón BJ, Horton MW, Meng D, Forai P, Huang YS, et al. GWAPP: a web application for genome-wide association mapping in *Arabidopsis*. *Plant Cell.* 2012; 24(12):4793–805. Epub 2013/01/02. <https://doi.org/10.1105/tpc.112.108068> PMID: 23277364; PubMed Central PMCID: PMC3556958.
23. Alonso-Blanco C, Blankestijn-de Vries H, Hanhart CJ, Koornneef M. Natural allelic variation at seed size loci in relation to other life history traits of *Arabidopsis thaliana*. *Proc Natl Acad Sci U S A.* 1999; 96(8):4710–7. Epub 1999/04/14. PMID: 10200327; PubMed Central PMCID: PMC384812.
24. Waese J, Fan J, Pasha A, Yu H, Fucile G, Shi R, et al. ePlant: Visualizing and Exploring Multiple Levels of Data for Hypothesis Generation in Plant Biology. *Plant Cell.* 2017; 29(8):1806–21. Epub 2017/08/16. <https://doi.org/10.1105/tpc.17.00073> PMID: 28808136; PubMed Central PMCID: PMC5590499.
25. Cole R, Peremysov V, Van Why S, Moussaoui I, Ketter A, Cool R, et al. A broadly conserved NERD genetically interacts with the exocyst to affect root growth and cell expansion. *J Exp Bot.* 2018; 69(15):3625–37. Epub 2018/05/04. <https://doi.org/10.1093/jxb/ery162> PMID: 29722827; PubMed Central PMCID: PMC6022600.
26. Higashiyama T, Yabe S, Sasaki N, Nishimura Y, Miyagishima S, Kuroiwa H, et al. Pollen tube attraction by the synergid cell. *Science.* 2001; 293(5534):1480–3. Epub 2001/08/25. <https://doi.org/10.1126/science.1062429> PMID: 11520985.
27. Okuda S, Tsutsui H, Shiina K, Sprunck S, Takeuchi H, Yui R, et al. Defensin-like polypeptide LUREs are pollen tube attractants secreted from synergid cells. *Nature.* 2009; 458(7236):357–61. <https://doi.org/10.1038/nature07882> PMID: 19295610.
28. Peaucelle A, Braybrook SA, Le Guillou L, Bron E, Kuhlemeier C, Hofte H. Pectin-induced changes in cell wall mechanics underlie organ initiation in *Arabidopsis*. *Curr Biol.* 2011; 21(20):1720–6. Epub 2011/10/11. <https://doi.org/10.1016/j.cub.2011.08.057> PMID: 21982593.
29. Peaucelle A, Louvet R, Johansen JN, Hofte H, Laufs P, Pelloux J, et al. *Arabidopsis* phyllotaxis is controlled by the methyl-esterification status of cell-wall pectins. *Curr Biol.* 2008; 18(24):1943–8. Epub 2008/12/23. <https://doi.org/10.1016/j.cub.2008.10.065> PMID: 19097903.
30. Elliott RC, Betzner AS, Huttner E, Oakes MP, Tucker WQ, Gerentes D, et al. *AINTEGUMENTA*, an *APETALA2*-like gene of *Arabidopsis* with pleiotropic roles in ovule development and floral organ growth. *The Plant Cell.* 1996; 8(2):155–68. <https://doi.org/10.1105/tpc.8.2.155> PMID: 8742707
31. Klucher KM, Chow H, Reiser L, Fischer RL. The *AINTEGUMENTA* gene of *Arabidopsis* required for ovule and female gametophyte development is related to the floral homeotic gene *APETALA2*. *The Plant Cell.* 1996; 8(2):137–53. <https://doi.org/10.1105/tpc.8.2.137> PMID: 8742706
32. Modrusan Z, Reiser L, Feldmann KA, Fischer RL, Haughn GW. Homeotic Transformation of Ovules into Carpel-like Structures in *Arabidopsis*. *The Plant Cell.* 1994; 6(3):333–49. <https://doi.org/10.1105/tpc.6.3.333> PMID: 12244239
33. Robinson-Beers K, Pruitt RE, Gasser CS. Ovule Development in Wild-Type *Arabidopsis* and Two Female-Sterile Mutants. *The Plant Cell.* 1992; 4(10):1237–49. <https://doi.org/10.1105/tpc.4.10.1237> PMID: 12297633
34. Schneitz K, Hulskamp M, Kopczak SD, Pruitt RE. Dissection of sexual organ ontogenesis: a genetic analysis of ovule development in *Arabidopsis thaliana*. *Development.* 1997; 124(7):1367–76. PMID: 9118807
35. Wilson ZA, Zhang DB. From *Arabidopsis* to rice: pathways in pollen development. *J Exp Bot.* 2009; 60(5):1479–92. Epub 2009/03/27. <https://doi.org/10.1093/jxb/erp095> PMID: 19321648.
36. Schaller GE, Bishopp A, Kieber JJ. The Yin-Yang of Hormones: Cytokinin and Auxin Interactions in Plant Development. *The Plant Cell.* 2015; 27(1):44–63. <https://doi.org/10.1105/tpc.114.133595> PMID: 25604447

37. Rameau C, Bertheloot J, Leduc N, Andrieu B, Foucher F, Sakr S. Multiple pathways regulate shoot branching. *Front Plant Sci.* 2014; 5:741. Epub 2015/01/30. <https://doi.org/10.3389/fpls.2014.00741> PMID: 25628627; PubMed Central PMCID: PMC4292231.
38. Thimann KV, Skoog F. Studies on the Growth Hormone of Plants: III. The Inhibiting Action of the Growth Substance on Bud Development. *Proc Natl Acad Sci U S A.* 1933; 19(7):714–6. Epub 1933/07/01. PMID: 16577553; PubMed Central PMCID: PMC4292231.
39. Domagalska MA, Leyser O. Signal integration in the control of shoot branching. *Nature Reviews Molecular Cell Biology.* 2011; 12:211. <https://doi.org/10.1038/nrm3088> PMID: 21427763
40. Lo SF, Yang SY, Chen KT, Hsing YI, Zeevaart JA, Chen LJ, et al. A novel class of gibberellin 2-oxidases control semidwarfism, tillering, and root development in rice. *Plant Cell.* 2008; 20(10):2603–18. Epub 2008/10/28. <https://doi.org/10.1105/tpc.108.060913> PMID: 18952778; PubMed Central PMCID: PMC4292231.
41. Silverstone AL, Mak PY, Martinez EC, Sun TP. The new RGA locus encodes a negative regulator of gibberellin response in *Arabidopsis thaliana*. *Genetics.* 1997; 146(3):1087–99. Epub 1997/07/01. PMID: 9215910; PubMed Central PMCID: PMC4292231.
42. Best NB, Hartwig T, Budka J, Fujioka S, Johal G, Schulz B, et al. nana plant2 Encodes a Maize Ortholog of the *Arabidopsis* Brassinosteroid Biosynthesis Gene DWARF1, Identifying Developmental Interactions between Brassinosteroids and Gibberellins. *Plant Physiol.* 2016; 171(4):2633–47. Epub 2016/06/12. <https://doi.org/10.1104/pp.16.00399> PMID: 27288361; PubMed Central PMCID: PMC4292231.
43. Best NB, Johal G, Dilkes BP. Phytohormone inhibitor treatments phenocopy brassinosteroid–gibberellin dwarf mutant interactions in maize. *Plant Direct.* 2017; 1(2). <https://doi.org/10.1002/pld3.9>
44. Wickson M, Thimann KV. The Antagonism of Auxin and Kinetin in Apical Dominance. *Physiologia Plantarum.* 1958; 11(1):62–74. <https://doi.org/10.1111/j.1399-3054.1958.tb08426.x>
45. Sachs T, Thimann KV. THE ROLE OF AUXINS AND CYTOKININS IN THE RELEASE OF BUDS FROM DOMINANCE. *American Journal of Botany.* 1967; 54(1):136–44. <https://doi.org/10.1002/j.1537-2197.1967.tb06901.x>
46. Yin Y, Wang Z-Y, Mora-Garcia S, Li J, Yoshida S, Asami T, et al. BES1 Accumulates in the Nucleus in Response to Brassinosteroids to Regulate Gene Expression and Promote Stem Elongation. *Cell.* 2002; 109(2):181–91. [https://doi.org/10.1016/S0092-8674\(02\)00721-3](https://doi.org/10.1016/S0092-8674(02)00721-3). PMID: 12007405
47. Foo E, Bullier E, Goussot M, Foucher F, Rameau C, Beveridge CA. The branching gene RAMOSUS1 mediates interactions among two novel signals and auxin in pea. *Plant Cell.* 2005; 17(2):464–74. Epub 2005/01/22. <https://doi.org/10.1105/tpc.104.026716> PMID: 15659639; PubMed Central PMCID: PMC4292231.
48. Shimizu-Sato S, Tanaka M, Mori H. Auxin-cytokinin interactions in the control of shoot branching. *Plant molecular biology.* 2009; 69(4):429–35. Epub 2008/11/01. <https://doi.org/10.1007/s11103-008-9416-3> PMID: 18974937.
49. Wang Y, Sun S, Zhu W, Jia K, Yang H, Wang X. Strigolactone/MAX2-induced degradation of brassinosteroid transcriptional effector BES1 regulates shoot branching. *Developmental cell.* 2013; 27(6):681–8. Epub 2013/12/29. <https://doi.org/10.1016/j.devcel.2013.11.010> PMID: 24369836.
50. Huang HY, Jiang WB, Hu YW, Wu P, Zhu JY, Liang WQ, et al. BR signal influences *Arabidopsis* ovule and seed number through regulating related genes expression by BZR1. *Mol Plant.* 2013; 6(2):456–69. Epub 2012/08/24. <https://doi.org/10.1093/mp/sss070> PMID: 22914576.
51. Nam YJ, Herman D, Blomme J, Chae E, Kojima M, Coppens F, et al. Natural Variation of Molecular and Morphological Gibberellin Responses. *Plant Physiol.* 2017; 173(1):703–14. Epub 2016/11/24. <https://doi.org/10.1104/pp.16.01626> PMID: 27879393; PubMed Central PMCID: PMC4292231.
52. Vu V, Verster AJ, Schertzberg M, Chuluunbaatar T, Spensley M, Pajkic D, et al. Natural Variation in Gene Expression Modulates the Severity of Mutant Phenotypes. *Cell.* 2015; 162(2):391–402. Epub 2015/07/18. <https://doi.org/10.1016/j.cell.2015.06.037> PMID: 26186192.
53. Lempe J, Balasubramanian S, Sureshkumar S, Singh A, Schmid M, Weigel D. Diversity of flowering responses in wild *Arabidopsis thaliana* strains. *PLoS Genet.* 2005; 1(1):109–18. Epub 2005/08/17. <https://doi.org/10.1371/journal.pgen.0010006> PMID: 16103920; PubMed Central PMCID: PMC4292231.
54. Curtis MD, Grossniklaus U. A gateway cloning vector set for high-throughput functional analysis of genes in planta. *Plant Physiol.* 2003; 133(2):462–9. <https://doi.org/10.1104/pp.103.027979> PMID: 14555774.
55. Clough SJ, Bent AF. Floral dip: a simplified method for *Agrobacterium*-mediated transformation of *Arabidopsis thaliana*. *Plant J.* 1998; 16(6):735–43. PMID: 10069079.
56. Davis TC, Jones DS, Dino AJ, Cejda NI, Yuan J, Willoughby AC, et al. *Arabidopsis thaliana* MLO genes are expressed in discrete domains during reproductive development. *Plant Reprod.* 2017; 30(4):185–95. Epub 2017/11/22. <https://doi.org/10.1007/s00497-017-0313-2> PMID: 29159588.

57. Nelson BK, Cai X, Nebenfuhr A. A multicolored set of in vivo organelle markers for co-localization studies in *Arabidopsis* and other plants. *Plant J.* 2007; 51(6):1126–36. <https://doi.org/10.1111/j.1365-313X.2007.03212.x> PMID: [17666025](https://pubmed.ncbi.nlm.nih.gov/17666025/).
58. Jones DS, Yuan J, Smith BE, Willoughby AC, Kumimoto EL, Kessler SA. MILDEW RESISTANCE LOCUS O Function in Pollen Tube Reception Is Linked to Its Oligomerization and Subcellular Distribution. *Plant Physiol.* 2017; 175(1):172–85. Epub 2017/07/21. <https://doi.org/10.1104/pp.17.00523> PMID: [28724621](https://pubmed.ncbi.nlm.nih.gov/28724621/); PubMed Central PMCID: [PMCPMC5580752](https://pubmed.ncbi.nlm.nih.gov/PMCPMC5580752/).
59. Christensen CA, King EJ, Jordan JR, Drews GN. Megagametogenesis in *Arabidopsis* wild type and the Gf mutant. *Sexual Plant Reproduction.* 1997; 10(1):49–64. <https://doi.org/10.1007/s004970050067> WOS:A1997WN66500008.
60. Alexander MP. Differential staining of aborted and nonaborted pollen. *Stain Technol.* 1969; 44(3):117–22. Epub 1969/05/01. PMID: [4181665](https://pubmed.ncbi.nlm.nih.gov/4181665/).
61. Kumar S, Stecher G, Tamura K. MEGA7: Molecular Evolutionary Genetics Analysis Version 7.0 for Bigger Datasets. *Mol Biol Evol.* 2016; 33(7):1870–4. Epub 2016/03/24. <https://doi.org/10.1093/molbev/msw054> PMID: [27004904](https://pubmed.ncbi.nlm.nih.gov/27004904/).
62. Felsenstein J. Confidence-Limits on Phylogenies—an Approach Using the Bootstrap. *Evolution.* 1985; 39(4):783–91. WOS:A1985APJ8100007. <https://doi.org/10.1111/j.1558-5646.1985.tb00420.x> PMID: [28561359](https://pubmed.ncbi.nlm.nih.gov/28561359/)